Correlations between *In Situ* Conductivity and Uniform-Height Epitaxial Morphology in Pb/Si(111)-(7 × 7)

M. Jałochowski,[1] R. Zdyb,[1] and M. C. Tringides[2]
[1]*Institute of Physics, M. Curie-Skłodowska University, Place M. Curie-Skłodowskiej 1, PL-20031 Lublin, Poland*
[2]*Department of Physics and Ames Laboratory–USDOE Iowa State University Ames, Ames, Iowa 50011, USA*
(Received 15 May 2015; revised manuscript received 16 November 2015; published 23 February 2016)

The growth of Pb on Si(111)-(7 × 7) at temperatures from 72 to 201 K has been investigated using *in situ* electrical resistivity measurements and scanning tunneling microscopy. For temperatures $T > 140$ K the specific resistivity $\rho(\theta)$ versus coverage θ shows an unusual "hump," instead of the expected monotonic decrease with θ. This novel result correlates well with the formation of uniform height eight-layer Pb islands and the superdiffusive motion of the wetting layer, despite the low temperatures. A model of the film resistivity as two resistors in series, the amorphous wetting layer and the crystalline islands, explains quantitatively the resistivity dependence on θ.

DOI: 10.1103/PhysRevLett.116.086101

The study of electronic transport in epitaxially grown metallic films of controllable morphology poses interesting questions about how nanoscale and mesoscale physics are interrelated. Some of the key nanoscale factors that determine electronic transport and the resistivity of the grown film are the growth mode (whether layer by layer or three dimensional), the density of atomic scale defects, and the quality of the interfaces. When the metallic film is growing on insulating substrates, one has ideal experimental realizations of theoretical models which describe the percolation transition; in particular, the experiments can be used to test the predicted critical behavior and identify the percolation universality class [1,2]. Even for substrates of high but finite resistivity the richness of epitaxial structures (ordered 2D metallic overlayers, 2D island networks, coexistence of amorphous and crystalline layers, etc.) offers additional possibilities to clarify the connection between nanoscale structure and mesoscale transport in ultrathin films. Furthermore, since the time to complete and the structural perfection of the metallic structures are related to the diffusion of the deposited atoms, *in situ* resistivity measurements are also sensitive to the type and range of mass transport in the system.

Recent low temperature epitaxial studies [3–10] of metal on semiconductor surfaces have shown a very surprising and unexpected film morphology. It was found that well below room temperature highly regular structures can be easily grown within the very short time of a few minutes. Pb/Si(111) has been the prototype system where such structures were observed. They were used to study electron confinement by mapping the confined electron level positions with island height. Surprisingly, it was also discovered that preferred island heights are observed at the minima of the electronic energy by using complementary techniques: STM, high-resolution LEED [9,10], and x-ray scattering [11,12]. The island electronic structure was investigated with angle resolved photoemission to confirm the variation of the electron energy levels with island height [13]. These observations have demonstrated the important role of quantum size effects (QSE) to control the grown morphology. The reason of the intense interest in Pb/Si(111) was the structural perfection and short completion time of the grown Pb islands, despite the very low temperatures. More recently, the interest in Pb/Si(111) has shifted to understanding the origin of the very unusual mass transport of the Pb adatoms which is responsible for the fast Pb nanostructure growth. A new type of collective diffusion was found, very different from classical random walk diffusion [14]. The height selectivity of perfect eight-layer Pb islands, with each containing on average $\sim 10^5$ atoms and the very fast buildup at ~180 K, are very novel dramatic results. *In situ* resistivity studies have also been carried out [15–19], but no quantitative analysis was applied to connect the uniform height island morphology with electron transport.

This raises the interesting question of whether the unusual growth and diffusion are also evident in the dependence of the film resistivity $\rho(\theta)$ on the deposited amount θ and if they are, what is the underlying conductivity mechanism? In the current work we answer positively both questions and show how these perfectly grown Pb islands can be used to further understand electron transport in an inhomogeneous system. Prior to the uniform eight-layer island distribution Pb forms an amorphous wetting layer which is expected to have higher resistivity than the crystalline Pb islands. However, instead of the monotonically decreasing $\rho(\theta)$ with θ observed in other studies where growth is layer by layer, a characteristic "hump" is observed with a maximum at intermediate coverage ~3 ML. The transport experiments are performed in real time [i.e., $\rho(\theta)$ is being measured while the atoms are deposited on the surface] and sense both the island height

uniformity and the very fast mass transport. The hump has not been observed in other systems when these conditions are absent. In addition, the layer underneath the islands, which was initially part of the wetting layer, transforms to crystalline islands, thus requiring the contact between the two resistors to be through the island perimeter and to depend on coverage as $\theta^{1/2}$ [20–22].

A simple model, which treats the high resistance wetting layer with the embedded crystalline low resistance Pb islands, as two resistors in series can account for the results. Because the Pb/Si(111) islands do not grow with one-layer but uniform eight-layer islands (over the whole coverage range 1 ML $< \theta <$ 8 ML), the deposited θ is used both to increase the length of the crystalline film resistor and also its "cross section." The combined effect of these opposing processes amounts to an increase of its effective resistivity ρ_{isl} at the hump maximum.

The resistivity experiments were performed in an ultra-high-vacuum system, equipped with a four-probe setup and a RHEED diffractometer. The substrates were n-doped (P) Si(111) wafers of ~500 Ω cm resistivity. The substrate could be cooled to ~70 K. The flux rate of approximately 1 ML/ min was calibrated using a quartz-crystal monitor and the strong RHEED intensity oscillations that develop during layer-by-layer growth [13,19,23].

The resistivity was measured by passing ac current of a few tenths of μA to two Mo clamps holding the crystal, and recording the voltage signal across two W sharp wires pressed against the Si crystal 6 mm apart. To prepare reproducible electrical contacts 1.5 ML of Au were initially deposited using a 4 mm wide mask and after annealing to 1000 K the Si(111)-(6×6)-Au reconstruction formed. Next, through the same mask 20 ML of Pb were deposited at 70 K, which grow layer by layer at this low temperature, so the grown film in the subsequent experiments made contact to these Pb precoated pads. The mask was removed during deposition in the resistivity experiments.

Figure 1(a) shows a 500×500 nm^2 STM image and Fig. 1(b) the corresponding island-height histogram obtained after Pb deposition of 4.2 ML at 190 K. The histogram peak positions and hence the island thicknesses are relative to the wetting layer measured in nm. Knowing that the islands are (111) oriented an integer number of monolayers H can be associated to the peaks. The linear fit (see inset) intercepts the ordinate at -0.376 ± 0.02 nm, which is the wetting layer thickness d_{WL} as measured by the STM. This thickness corresponds to 1.32 ± 0.09 ML of the Pb(111) density, in good agreement with 1.2 ML, the value extracted from the variation of the Pb(111) diffraction spot intensity versus θ in surface x-ray experiments [21,22].

Figure 1(a) also shows that the majority of the eight-layer islands have clear tops because the highly mobile wetting layer moves only to unstable height islands (of a height less than eight layers) converting them to superstable eight-layer islands. A few of the eight-layer islands have

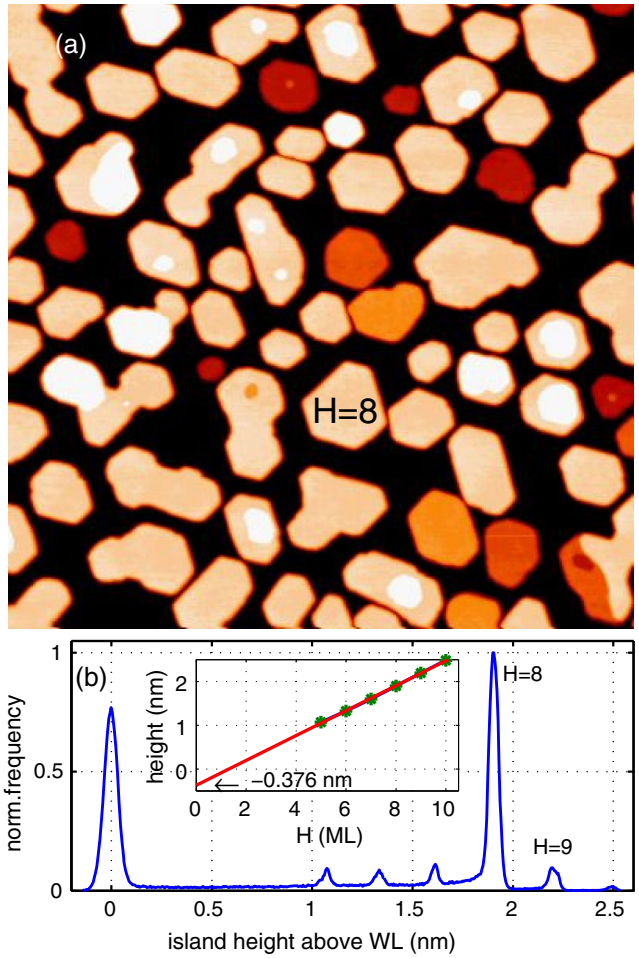

FIG. 1. (a) 500×500 nm^2 STM image. (b) The corresponding island-height histogram. The experiment was carried out at 190 K with 4.2 ML deposited. The tunneling bias was +3.5 V and the tunneling current was 0.28 nA.

single-layer islands at their center, showing that some material has fallen directly on top. Since it was not added at the island edges it confirms that the superdiffusive motion of the wetting layer is selective and targets only unstable height islands.

Figure 2 presents the *in situ* specific resistivity at temperatures from 72 to 201 K. The behavior of Pb ultrathin films deposited at 72 K was studied thoroughly before, no islands form but continuous film [11,17,21]. As shown, the wetting layer thickness is a strong function of growth temperature with 7 ML at 18 K, decreasing to 1.27 ML at 190 K before crystallization [23].

Three regimes of the $\rho(\theta)$ dependence can be identified. In the first regime, up to θ_{WL}, $\rho(\theta)$ is independent of T and decreases rapidly to ~170 $\mu\Omega$ cm. The deposited material forming the wetting layer preserves the (7×7) reconstruction [22]. Since shortly after the first eight-layer islands grow at θ_{WL} the resistance of the sample is approximately constant (the few eight-layer islands that have nucleated do not contribute to the resistance) the

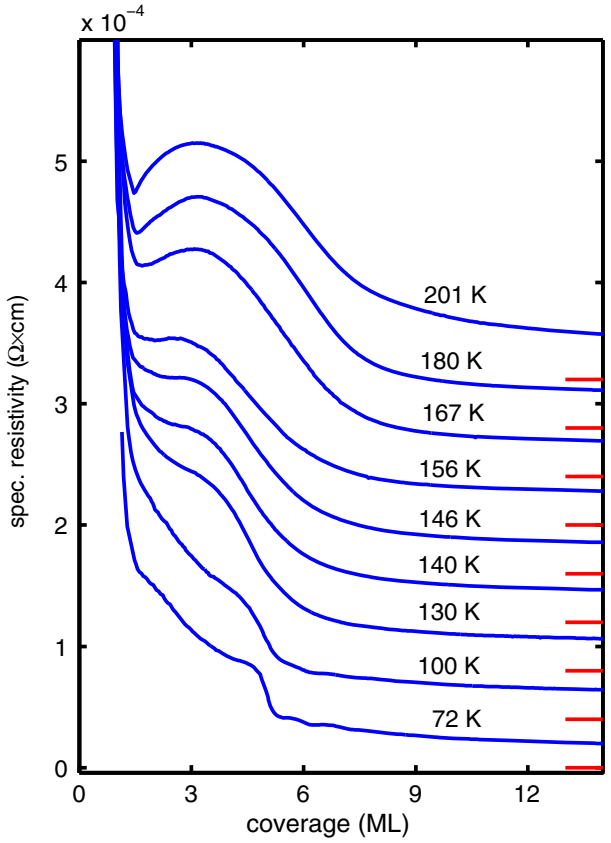

FIG. 2. Specific resistivity during the growth of Pb on Si(111)-(7 × 7) substrate as a function of Pb deposited amount with the substrate temperature ranging from 72 K −201 K. The curves are shifted vertically with the origin of each curve shown to the right as a straight segment.

average specific resistivity $\rho(\theta)$ increases because it is proportional to the product of resistance R with θ. The transition is very sharp, consistent with height uniformity and superdiffusive kinetics. In the second regime the well-developed hump is present for $T > 140$ K signifying the onset of uniform height island growth [9,10] with maximum at average deposition ∼3 ML. Deposition at lower $T < 140$ K results first in the formation of a Pb layer with high $\rho(\theta)$ which is highly disordered as seen from the absence of diffraction oscillations [22,23].

In the third regime, $\theta > 8$ ML, all curves behave in the same manner. Moreover, for fixed thickness, as expected for metals, the specific resistivity increases with temperature. This is clearly evident at the right end of the curves in Fig. 2, where straight segments represent the origin for each of the curves. In this region studied in detail previously [19], at the lowest temperatures $\rho(\theta)$ follows thickness dependent modulation, since crystalline Pb(111) continuous atomically flat films form. The presence of QSE above 150 K clearly shows that after film crystallization the electrons are very efficiently reflected from the substrate-film interface, which further supports the previous conclusion that the bottom layer of the island has transformed from amorphous to crystalline.

In the following a model, which demonstrates how the growth mode correlates with the shape of the specific resistivity $\rho(\theta)$ hump, is presented. The model is applicable when uniform height Pb(111) islands grow ($170 < T < 220$ K) [9], with a very narrow eight-layer height distribution.

The system can be modeled by a network of areas with low ρ_{isl} for the islands embedded in a "sea" of the wetting layer of higher ρ_{WL}. Islands of fixed H layers [the island height is Hd_0 where d_0 is the Pb(111) step height] emerge after $\theta > \theta_{\mathrm{WL}}$. The Pb amount in the islands is $\theta - \theta_{\mathrm{WL}}$ so the substrate relative area covered with islands is given by $\beta = (\theta - \theta_{\mathrm{WL}})/(\theta_H - \theta_{\mathrm{WL}})$, which grows linearly with θ, until the full H-layer film with coverage θ_H is completed. The relative area of the wetting layer shrinks correspondingly proportional to $(1 - \beta)$. Because of lower conductivity of the wetting layer, in comparison to the conductivity of the islands, the current flux concentrates in the islands so the system can be modeled as two resistors in a series. The area covered with the wetting layer is represented by resistor R_{WL} with high resistance, and the area covered with the islands by resistor R_{isl}, with low resistance. The length of R_{isl} is proportional to the perimeter of the growing islands and is given by $\beta^{1/2}$, which is limiting contact between the wetting layer and the islands. The corresponding resistances in series for a 1×1 cm^2 square is obtained using the basic resistance equation $R = \rho L/A$, for a layer of length L and cross section A:

$$R_{\mathrm{WL}}(\theta) = \rho_{\mathrm{WL}}[1 - \sqrt{(\theta - \theta_{\mathrm{WL}})/(\theta_H - \theta_{\mathrm{WL}})}]/(\theta_{\mathrm{WL}} d_0), \tag{1}$$

$$R_{\mathrm{isl}}(\theta) = \rho_{\mathrm{isl}}[\sqrt{(\theta - \theta_{\mathrm{WL}})/(\theta_H - \theta_{\mathrm{WL}})}]/(\theta_H d_0). \tag{2}$$

These equations are valid for $\theta_{\mathrm{WL}} \le \theta < \theta_H$ and the average specific resistivity $\rho(\theta)$ of the sample is given by

$$\rho(\theta) = \rho_{\mathrm{WL}} \frac{\theta}{\theta_{\mathrm{WL}}} \left[1 - \sqrt{\frac{\theta - \theta_{\mathrm{WL}}}{\theta_H - \theta_{\mathrm{WL}}}}\right] + \rho_{isl} \frac{\theta}{\theta_H} \sqrt{\frac{\theta - \theta_{\mathrm{WL}}}{\theta_H - \theta_{\mathrm{WL}}}}. \tag{3}$$

The coverage of the amorphous layer, when islands start to form, remains constant and equals θ_{WL}. Equation (3) can be used to fit the experimental data of Fig. 2 with four parameters obtained independently, from data outside of the hump region. The specific resistivity of the islands ρ_{isl} of H layers can be derived using the Fuchs-Sondheimer formula, where p *is* the specularity parameter at the film-vacuum interface, q is the specularity parameter at the film-substrate interface, l is the electron mean free path, and ρ_∞ is the Pb bulk resistivity

$$\rho(H) = \rho_\infty \left[1 + \frac{3}{8}\left(1 - \frac{p+q}{2}\right)\frac{l}{Hd_0}\right], \qquad (Hd_0 \gg l). \tag{4}$$

First, the parameters $\rho_\infty = 21.3\,\mu\Omega$cm and $[1-(p+q)/2]l = 4.99$ nm are extracted from Eq. (4) by fitting the resistivity data of Fig. 2 over the higher coverage range 10 ML $< \theta <$ 20 ML (and $T = 180$ K) when the resistivity curve $\rho(\theta)$ becomes flat. Next, these values are used as input to Eq. (4) to calculate the resistivities for given island height H. I.e., $\rho(H = 8) = 40.6\ \mu\Omega\,$cm and for $\rho(H = 7) = 43.6\ \mu\Omega\,$cm, relevant when the hump develops. It was shown in Ref. [19] that Eq. (4) is applicable for metal films of few layers.

Examples of the fit of the hump according to Eq. (3) for $\rho(\theta)$ measured at 180 K are shown in Fig. 3. It shows two calculated curves for islands with a height equal to $H = 7$ and $H = 8$. Clearly the hump is reproduced in the fit and the experimental curve lies closely between the two curves. It is intriguing that the rather complex shape can be fitted with all the parameters fixed from information unrelated to the hump. It is also surprising that the extracted resistivity of the amorphous (but highly compressed) wetting layer $\rho_{\mathrm{WL}} = 170\ \mu\Omega\,$cm is only 3.9 times larger than the resistivity of the eight-layer crystalline islands, despite being disordered and nonperiodic; but this is in very good agreement with the metallic character of the wetting layer as deduced from the proximity effect studied at 0.3 K between the superconducting Pb islands and the wetting layer [24]. Interestingly, the best fit was obtained for

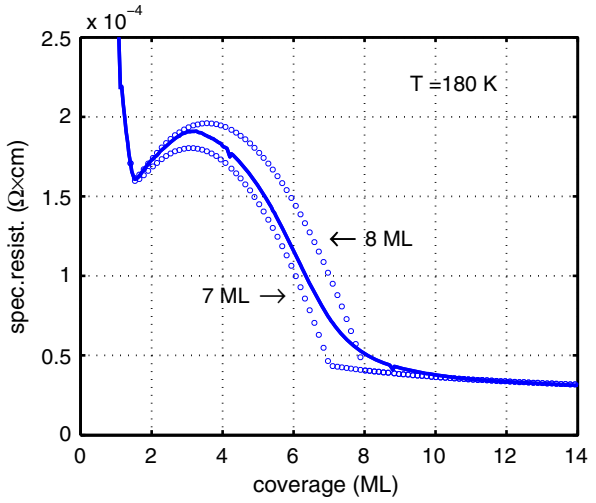

FIG. 3. Experimental specific resistivity (continuous line) measured at 180 K, and calculated (open dots) according to Eq. (3) with $H = 7$ (left) and $H = 8$ (right). The parameters $\rho(H = 8) = 40.6\ \mu\Omega\,$cm and for $\rho(H = 7) = 43.6\ \mu\Omega\,$cm are from Eq. (4) and $\rho_{\mathrm{WL}} = 170\ \mu\Omega\,$cm at θ_{WL}. The sharp coverage transition at $\theta_{\mathrm{WL}} = 1.4$ ML where the wetting layer converts to crystalline islands is in agreement with the result of other experiments.

$\theta_{\mathrm{WL}} = 1.40 \pm 0.10$ ML. This estimate of the wetting layer coverage θ_{WL} is consistent with the values extracted from Fig. 1 and the value extracted from the variation of the Pb(111) diffraction intensity versus the deposited amount in the surface x-ray experiments [21,22].

The description of the resistance of the system as the sum of two resistors in series can be rationalized. Because the Pb/Si(111) film grows with uniform eight-layer islands, the amount being deposited θ has opposing effects on the film resistance; i.e., it is used both to increase the length and cross section of the resistor. This amounts first to an increase of its effective resistivity followed by the generation of the hump. No hump is observed at higher temperature or higher coverage, because for these conditions height selectivity due to QSE is not seen: the "confining wells" have larger widths and therefore the electron level spacing decreases with island height. This reduces the difference of the electron energy and therefore the relative stability between islands of adjacent heights. The unusual $\rho(\theta)$ trace is only seen when the conditions of sharp height selectivity and fast collective diffusion are present [25]. It is not seen in resistivity experiments during Pb deposition on other substrates [Pb/Si(111)-Au(6×6) [13] or Ag/Si(111)-(7×7)] [19] where these two conditions are absent.

In the current experiments there is an additional advantage because the relation between transport and growing morphology is established from real time experiments with the resistance measured as the atoms are deposited on the surface. This adds more possibilities when compared to measurements on a finite set of samples, at discrete coverages, to determine the conductivity of the film. The real time measurements increase the number of experimental parameters that control the percolation transition. Because the voltage drop is recorded in real time the experiments relate better morphological changes to electronic transport, by being sensitive not only to the connectivity in the film, but to the mass transport to build the nanoscale structures, the controlling kinetic barriers, and the diffusion time.

In summary, *in situ* conductivity measurements have been used to correlate nanoscale morphological changes in Pb/Si(111) to mesoscale electron transport. Normally, the resistivity is expected to drop monotonically with the deposited Pb amount if growth is layer by layer. Because of the height island uniformity and the very sharp transition from the amorphous wetting layer to the islands an unusual hump is observed in $\rho(\theta)$. A quantitative fit was possible by assuming the wetting layer and the islands were resistors in series. Their electrical contact was defined by the island perimeter, thus confirming the conversion of the bottom island layer to crystalline Pb(111). The hump is consistent with the superdiffusive kinetics that once a critical coverage θ_{WL} is deposited the islands emerge very fast out of the wetting layer. Fit to

$\rho(\theta)$ using parameters obtained in a different growth regime where growth is layer by layer, confirm the predictive power of the analysis.

Part of this work was supported by the U.S. Department of Energy (DOE), Office of Science, Basic Energy Sciences, Materials Science and Engineering Division, under Contract No. DEAC0207CH11358, and part was supported by National Science Centre, Poland, under Grant No. 2014/13/B/ST5/04442. We are grateful to M. Stróżak for his participation in the measurements and for technical assistance.

[1] J. P. Clerc, G. Giraud, J. M. Laugier, and J. M. Luck, Adv. Phys. **39**, 191 (1990).
[2] D. J. Bergman and D. Stroud, Solid State Phys. **46**, 147 (1992).
[3] W. B. Su, S. H. Chang, W. B. Jian, C. S. Chang, L. J. Chen, and T. T. Tsong, Phys. Rev. Lett. **86**, 5116 (2001).
[4] L. Gavioli, K. R. Kimberlin, M. C. Tringides, J. F. Wendelken, and Z. Zhang, Phys. Rev. Lett. **82**, 129 (1999).
[5] R. Otero, A. L. Vazquez de Parga, and R. Miranda, Phys. Rev. B **66**, 115401 (2002).
[6] K. L. Man, Z. Q. Qiu, and M. S. Altman, Phys. Rev. Lett. **93**, 236104 (2004).
[7] D. A. Fokin, S. I. Bozhko, V. Dubost, F. Debontridder, A. M. Ionov, T. Cren, and D. Roditchev, Phys. Status Solidi (c) **7**, 165 (2010).
[8] V. Fournee, H. R. Sharma, M. Shimoda, A. P. Tsai, B. Unal, A. R. Ross, T. A. Lograsso, and P. A. Thiel, Phys. Rev. Lett. **95**, 155504 (2005).
[9] K. Budde, E. Abram, V. Yeh, and M. C. Tringides, Phys. Rev. B **61**, R10602 (2000).
[10] M. C. Tringides, M. Jalochowski, and E. Bauer, Phys. Today **60**, 50 (2007).
[11] C. A. Jeffrey, E. H. Conrad, R. Feng, M. Hupalo, C. Kim, P. J. Ryan, P. F. Miceli, and M. C. Tringides, Phys. Rev. Lett. **96**, 106105 (2006).
[12] H. Hong, C. M. Wei, M. Y. Chou, Z. Wu, L. Basile, H. Chen, M. Holt, and T. C. Chiang, Phys. Rev. Lett. **90**, 076104 (2003).
[13] M. Jalochowski, H. Knoppe, G. Lilienkamp, and E. Bauer, Phys. Rev. B **46**, 4693 (1992).
[14] M. C. Tringides, M. Hupalo, K. L. Man, M. M. T. Loy, and M. S. Altman, *Wetting layer super-diffusive motion and QSE growth in Pb/Si in Nanophenomena at Surfaces: Exotic Condensed Matter Properties*, edited by M. Michailov (Springer, New York, 2011).
[15] D. Lukermann, H. Pfnür, and C. Tegenkamp, Phys. Rev. B **82**, 045401 (2010).
[16] M. Yamada, T. Hirahara, and S. Hasegawa, Phys. Rev. Lett. **110**, 237001 (2013).
[17] K. Wang, X. Zhang, M. M. T. Loy, and X. Xiao, Surf. Sci. **602**, 1217 (2008).
[18] O. Pfennigstorf, A. Petkova, Z. Kallassy, and M. Henzler, Eur. Phys. J. B **30**, 111 (2002).
[19] M. Jałochowski and E. Bauer, Phys. Rev. B **38**, 5272 (1988).
[20] K. A. Edwards, P. B. Howes, J. E. MacDonalds, T. Hibma, T. Bootsma, and M. A. James, Surf. Sci. **424**, 169 (1999).
[21] R. Feng, E. H. Conrad, C. Kim, P. F. Miceli, and M. C. Tringides, Physica (Amsterdam) **357B**, 175 (2005).
[22] R. Feng, E. H. Conrad, M. C. Tringides, C. Kim, and P. F. Miceli, Appl. Phys. Lett. **85**, 3866 (2004).
[23] M. Jałochowski, M. Hoffmann, and E. Bauer, Phys. Rev. B **51**, 7231 (1995).
[24] L. Serrier-Garcia, J. C. Cuevas, T. Cren, C. Brun, V. Cherkez, F. Debontridder, D. Fokin, F. S. Bergeret, and D. Roditchev, Phys. Rev. Lett. **110**, 157003 (2013).
[25] See Supplemental Material at http://link.aps.org/supplemental/10.1103/PhysRevLett.116.086101, which includes Refs. [26,27], for experimental conditions necessary to observe the specific resistivity traces in the current experiments are briefly described.
[26] S. Heun, J. Bange, R. Schad, and M. Henzler, J. Phys. Condens. Matter **5**, 2913 (1993).
[27] M. Jałochowski, M. Hoffman, and E. Bauer, Phys. Rev. Lett. **76**, 4227 (1996).